

Three-dimensional Electrocardiographically Gated Variable Flip Angle FSE Imaging for MR Angiography of the Hands at 3.0 T: Initial Experience¹

Ruth P. Lim, MBBS, M.Med, FRANZCR
Pippa Storey, PhD
Iliyana P. Atanasova, MS
Jian Xu, BS
Elizabeth M. Hecht, MD
James S. Babb, PhD
David R. Stoffel, ARMRIT
Hugo Chang, BS
Kellyanne McGorty, RT
Qun Chen, PhD
Henry Rusinek, PhD
H. Michael Belmont, MD
Vivian S. Lee, MD, PhD, MBA

After institutional review board approval and informed consent were obtained for this HIPAA-compliant investigation, a three-dimensional electrocardiographically gated variable flip angle (VFA) fast spin-echo magnetic resonance (MR) angiography technique was evaluated as an unenhanced method for imaging hand arteries in 13 subjects (including four patients) at 3.0 T; this included evaluation of vessel visualization with warming and cooling in seven subjects. Examinations were evaluated for image quality and vessel conspicuity. Clear separation of arteries from veins was achieved in all subjects, with excellent vessel conspicuity and depiction of stenoses. Warming improved vessel visualization in healthy volunteers. VFA MR angiography is a high-spatial-resolution technique that enables the assessment of vascular reactivity in response to temperature challenge.

© RSNA, 2009

¹ From the Department of Radiology (MRI), New York University Langone Medical Center, 530 First Ave, Basement Schwartz Bldg, New York, NY 10016 (R.P.L., P.S., I.P.A., E.M.H., J.S.B., D.R.S., K.M., Q.C., H.R., V.S.L.); Department of Rheumatology, NYU Hospital for Joint Diseases, New York, NY (H.M.B.); and MR R&D Collaboration, NYU Center for Biomedical Imaging, Siemens Medical Solutions, New York, NY (J.X., H.C.). Received February 15, 2009; revision requested March 19; revision received March 27; accepted April 3; final version accepted April 14. Address correspondence to R.P.L. (e-mail: ruth.lim@nyumc.org).

© RSNA, 2009

Imaging is vital in the work-up and management of vascular hand abnormalities, including thromboembolic disease, vasculitides, trauma, and vascular malformations. The standard of reference for hand evaluation is digital subtraction angiography (1). However, digital subtraction angiography has associated risks of puncture site complications, ionizing radiation, and iodine nephrotoxicity and can also be a painful procedure for patients. In addition, vasodilators are frequently required for optimal visualization of the small arteries of the hand, which are highly reactive to noxious stimuli (2). Contrast material-enhanced magnetic resonance (MR) angiography has been advocated as a suitable noninvasive alternative (3–5), but small vessel caliber, relatively slow arterial flow, and short arteriovenous transit times can hamper arterial visualization (1,6). Attempts to shorten imaging times can compromise spatial resolution or signal-to-noise ratio.

An unenhanced technique is desirable, particularly in patients with vasculitides or concurrent renovascular disease, in whom renal function may be compromised and nephrogenic systemic fibrosis becomes a potential clinical concern (7). Time-of-flight and phase-contrast techniques have been reported (8) but are limited by long imaging times and limited coverage (1).

Advances in Knowledge

- Three-dimensional electrocardiographically gated variable flip angle (VFA) fast spin-echo (FSE) MR angiography of the hands yields high-spatial-resolution images with good arterial conspicuity, including visualization of the digital arteries.
- Without the need for injected contrast material, this technique can be repeated and can consistently provide arterial phase images without venous signal “contamination.”
- The noninvasive nature of the technique enables evaluation of the hand vasculature at baseline and after temperature challenge.

An electrocardiographically gated spin-echo-based MR angiographic technique was initially described by Wedeen et al (9) and was later adapted into a three-dimensional (3D) single-shot fast spin-echo (FSE) technique by Miyazaki et al (10) on the basis of the principle that black blood images can be obtained in fast-flowing blood with spin-echo sequences.

Promising results have been obtained with this technique for the lower extremities (11); however, vessel blur that is related to echo train length and relative insensitivity to slow arterial flow could limit its use in the hand. Use of a variable flip angle (VFA) FSE-based MR angiographic technique, sampling perfection with application of optimized contrasts using different flip angle evolutions, or SPACE (12), has been described. The use of a VFA technique facilitates shorter inter-echo spacing and readout duration with subsequently decreased vessel blurring; more accurate sampling of peak and slowest flow in systole and diastole, respectively; and decreased radiofrequency deposition compared with a constant flip angle single-shot FSE approach (13).

We hypothesize that VFA MR angiography will enable high-spatial-resolution, entirely noninvasive evaluation of the arteries of the hand. The primary purpose of this study was to develop and evaluate the feasibility of the VFA MR angiographic technique for hand MR angiography at 3.0 T. A secondary aim was to use the technique to evaluate the effects of temperature challenge on visualization of the small vessels of the hand.

Materials and Methods

Two authors (J.X. and H.C.) are employees of Siemens Medical Solutions, the manufacturer of the MR imaging system used in this study. The other authors

Implication for Patient Care

- Three-dimensional electrocardiographically gated VFA FSE MR angiography of the hands provides a noninvasive means of evaluating arterial anatomy without the need for injected contrast material.

(who are not Siemens employees) had control of the data and information that might present a conflict of interest for the employee authors.

Subjects

This prospective technical development study was approved by the institutional ethics committee of New York University Langone Medical Center and was compliant with the Health Insurance Portability and Accountability Act. Informed consent was obtained from all subjects. Unenhanced hand MR angiographic examinations were performed in 13 subjects aged 26–67 years (mean age, 47.3 years). There were six men with a mean age of 47.8 years (range, 26–62 years) and seven women with a mean age of 46.9 years (range, 34–67 years). Nine of the subjects were healthy volunteers (five men aged 26–62 years [mean age, 46.8 years] and four women aged 34–41 years [mean age, 37.5 years]). Four of the subjects were patients (one man aged 53 years and three women aged 45–67 years [mean age, 59.3 years]); all patients had a history of limited scleroderma and secondary Raynaud disease. A total of 16 hands (nine right, seven left) were imaged; 10 hands were imaged without temperature challenge.

A subset of seven subjects (two men

Published online before print

10.1148/radiol.2531090290

Radiology 2009; 252:874–881

Abbreviations:

FSE = fast spin echo
MIP = maximum intensity projection
3D = three-dimensional
VFA = variable flip angle

Author contributions:

Guarantor of integrity of entire study, R.P.L.; study concepts/study design or data acquisition or data analysis/interpretation, all authors; manuscript drafting or manuscript revision for important intellectual content, all authors; manuscript final version approval, all authors; literature research, R.P.L., I.P.A., V.S.L.; clinical studies, R.P.L., P.S., I.P.A., J.X., E.M.H., H.C., H.M.B.; statistical analysis, R.P.L., J.X., J.S.B.; and manuscript editing, R.P.L., P.S., E.M.H., J.S.B., H.C., Q.C., H.R., V.S.L.

Funding:

This work supported by the National Institutes of Health (grant HL092439).

See Materials and Methods for pertinent disclosures.

aged 39 and 53 years and five women aged 34–66 years [mean age, 44.8 years]) underwent imaging after temperature challenge. Of the subjects in this subset, four were healthy volunteers and three were patients. Two volunteers reported a history of digital color change with exposure to cold, and two volunteers had no history of cold sensitivity. Seven hands were imaged with temperature challenge. One volunteer's hand was imaged twice—once without temperature challenge and once with temperature challenge—resulting in a total of 16 hands imaged overall.

The average heart rate was 72.9 beats per minute (range, 62–90 beats per minute), with irregular rhythm noted in two patients (atrial fibrillation and frequent premature ventricular contractions in one patient each).

MR Imaging Protocol

Imaging was performed at 3.0 T (Trio; Siemens, Erlangen, Germany), with subjects imaged in the prone position with arms raised above the head in a “Superman” posture (two volunteers) for simultaneous bilateral hand imaging and in the lateral decubitus position for imaging of the contralateral hand (11 subjects). Foam wedges and a custom-designed hand holder were used to minimize subject motion. Central electrocardiographic gating was used in all subjects. Examinations were tailored to hand size and to the surface coil employed. For prone imaging, a six-element surface phased-array coil was used. For lateral decubitus imaging, a 12-channel head coil was used for larger hands and an eight-channel knee coil was used for smaller hands. VFA MR angiography is subtraction based, developed from the 3D single-shot FSE MR angiographic technique, in which fast arterial flow (flow void) from systolic images is subtracted from slow arterial flow that appears bright on diastolic images (14). With cancellation of venous and background tissue, which are similar on both systolic and diastolic images, a bright-blood MR angiogram is obtained (Fig 1).

An oblique coronal acquisition covering the entire hand in the plane of the palm and fingers was performed with a

left-to-right phase-encoding direction. Imaging parameters were as follows: repetition time, two R-R intervals; effective echo time, 10 msec; variable flip angle; interecho spacing, 3.3 msec; voxel size, $0.7 \times 0.8 \times 1\text{--}2$ mm; bandwidth, 745 Hz/voxel; 26–64 partitions (average, 38.5 partitions); average acquisition time, 2 minutes 52 seconds (1 minute 40 seconds to 4 minutes 30 seconds); and field of view, $240\text{--}280 \times 156 \times 252$ mm. To minimize readout duration, two echo trains per section were employed, for 43 echoes per train with the use of parallel imaging (generalized autocalibrating partially parallel acquisitions, acceleration factor 2–3) (15). Owing to the use of half-Fourier acquisition in the phase-encoding direction, the echo train duration was 73 msec. Centric encoding was employed. Although earlier studies using a single-shot FSE-based approach incorporated additional flow spoiling to achieve the necessary degree of flow sensitivity for peripheral MR angiography (11,16), no additional spoiling was required with our technique because VFA MR angiography is intrinsically more flow sensitive than single-shot FSE because of the lower flip angles of its refocusing pulses (17,18).

For systolic imaging, trigger delays were based on a two-dimensional gradient-echo phase-contrast scout sequence with velocity encoding of 40 cm/sec, enabling identification of the optimal trigger time, coinciding with peak systolic flow based on a velocity-versus-time curve (Mean Curve, Leonardo; Siemens). A

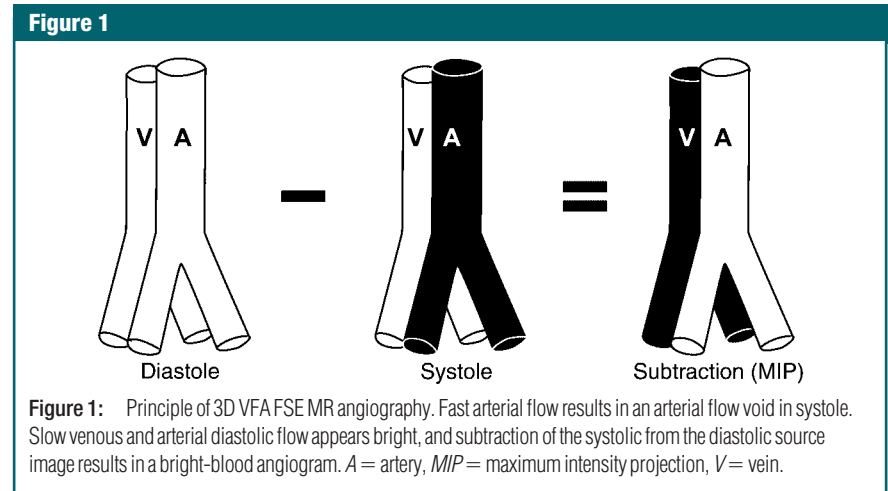
0-msec trigger delay was used for diastolic imaging because it coincided with end diastole when velocity-versus-time curves were reviewed for all subjects. Systolic and diastolic acquisitions were acquired consecutively without pause.

For the subjects who underwent temperature challenge, images were acquired after cooling with hand immersion in cold water (for 2 minutes at 10°C) for healthy volunteers and after sitting in a temperature-controlled room (13°C) for 20 minutes for patients. Healthy volunteers and patients were then imaged a second time after warming for 10 minutes with saline bags heated to 50°C .

Subjects were questioned (I.P.A., D.R.S.) with regard to whether the imaging position was comfortable or uncomfortable at the conclusion of imaging and were asked to describe the nature of their discomfort if applicable. Imaging time for each MR angiographic acquisition, average heart rate, and presence of arrhythmias were recorded for each subject (R.P.L.).

Image Analysis

Subtracted 3D data sets were evaluated by two radiologists (R.P.L. and E.M.H., with 3 and 6 years of experience with vascular MR image interpretation, respectively) in consensus on a workstation (Leonardo, Siemens) and were reviewed by using multiplanar reconstruction and MIP. Overall image quality was assessed by using a four-point Likert scale, where a score of 0 indicated nondiagnostic; a score of 1, poor; a score of 2, satisfactory;



and a score of 3, excellent image quality. The number of vascular segments (palmar arches and metacarpal, common digital, radialis indicis, princeps pollicis, and proper digital arteries) present and vessel segment conspicuity (0 = nondiagnostic; 1 = poor, impairing diagnosis; 2 = suboptimal without diagnostic impairment; 3 = good arterial signal intensity) were recorded (19). For proper digital arteries, the number of digital arteries visible to the terminal third was recorded. Visualization of terminal nutrient arteries was also recorded on a per-subject basis. The presence of venous signal (0 = absent; 1 = present, not limiting interpretation; 2 = present, affecting image interpretation) was assessed. Motion artifact was graded separately for palmar (palmar arches and metacarpal and common digital arteries) and digital (radialis indicis, princeps pollicis, and proper digital arteries) segments as follows: a grade of 0 indicated absent; a grade of 1, present, not affecting image interpretation; a grade of 2, present, affecting image interpretation; and a grade of 3, severe, rendering images nondiagnostic. Pathologic conditions and anatomic variants were recorded qualitatively.

In subjects who underwent temperature challenge, images were reviewed for image quality, number of vessel segments, and segment conspicuity for both cool and warm image data sets. Any change in the number of visualized segments between cool and warm imaging was recorded. The diameter of the superficial palmar arch was measured in six subjects who underwent provocative testing, and the diameter of the terminal radial artery was measured in one subject in whom the superficial palmar arch was not visualized. Arterial caliber was measured in millimeters at the same positions on magnified coronal subtraction MIP images, with cool and warm images viewed side-by-side for each subject.

Statistical Analysis

The number of vessel segments visualized, systolic and diastolic acquisition times, and segment conspicuity scores were summarized as means \pm standard deviations. An analysis of segmental conspicuity on the basis of segment location, comparing palmar

vessels (palmar arches, metacarpal and common digital arteries) with digital vessels (radialis indicis, princeps pollicis, and proper digital arteries), was performed (J.S.B.). Generalized estimating equations based on a binary logistic regression model were used to compare palmar and digital vessels and to derive confidence intervals for the percentage of vessels that could be expected to show excellent conspicuity. The dependent variable was the binary indicator identifying vessels that received a conspicuity score of 3. The model included hand (left vs right) and vessel position (palmar vs digital) as classification factors. The correlation structure was modeled by assuming that observations correlated only when derived for the same patient, with the strength of the correlation dependent on whether vessels were from the same hand. Software (SAS, version 9.0; SAS Institute, Cary, NC) was used for statistical computations. Results were declared significant when associated with a *P* value of less than .05.

Results

VFA MR angiography was well tolerated, with successful completion of the MR angiographic examination in all cases. Image acquisition in the lateral decubitus position was comfortable for all but one subject, who reported pain in the dependent shoulder due to positional impingement. Both subjects who were imaged in the prone position reported bilateral arm stiffness secondary to immobility and prolonged bilateral arm extension, with paresthesias also noted in one subject toward the end of the examination. This position, however, enabled bilateral hand examination in the same acquisition time.

Baseline Imaging without Temperature Challenge

Image quality was excellent for six subjects and was satisfactory for four, with no images considered poor quality or nondiagnostic. One hundred fifty-eight vascular segments were visualized in 10 hands without temperature challenge: 19 palmar arch, 30 common digital, 23 palmar metacarpal, 10 princeps pollicis, nine arteria radialis indicis, and 67 proper digital artery segments. The mean number

of segments visualized per hand was 15.8 ± 2.3 (standard deviation). Fifty-seven (85%) of the 67 proper digital arteries were visualized to their terminal third. High in-plane resolution enabled visualization of terminal nutrient arteries in three subjects (Fig 2).

There was high vessel segment conspicuity, with scores as follows: palmar arch, 2.9 ± 0.5 (a score of 3 is consistent with good arterial signal intensity); common digital and metacarpal arteries, 2.9 ± 0.3 ; arteria radialis indicis and princeps pollicis arteries, 2.5 ± 0.6 ; and proper digital arteries, 2.7 ± 0.6 . When segments were stratified into palmar (proximal) and digital (distal) vessels, 66 (92%) of the 72 palmar vessels received excellent conspicuity scores (95% confidence interval: 72.5%, 97.9%). For digital vessels, excellent conspicuity was recorded in 59 (69%) of 86 segments (95% confidence interval: 48.0%, 83.8%). The difference between palmar and digital vessel conspicuity was statistically significant (*P* = .01). The mean conspicuity score was 2.9 ± 0.34 for proximal vessels and 2.6 ± 0.60 for distal vessels.

There was no venous “contamination” recorded for any subject (score of 0 for all subjects). Mild motion artifact was present in the palmar segments of five subjects but did not affect image interpretation. For digital segments, motion artifact was noted in five subjects, limiting image interpretation in two. One proper digital artery segment was partially excluded from the imaging field of view.

Anatomic variations included a persistent median artery (Fig 3). The one patient with scleroderma imaged at baseline had an abnormal image, with 12 vessel segments visualized overall—fewer than for volunteers—and vessel tortuosity and irregularity were noted.

Temperature Challenge

Provocative testing of seven subjects yielded differences in the number of visualized segments for volunteers versus patients. For healthy volunteers, the transition from cold to warm increased the number of visualized segments, whereas for patients, minimal change was observed. With regard to vessel caliber, an increase in caliber was noted in three vol-

unteers and one patient, with no change for the remaining subjects. These results are summarized graphically in Figure 4.

All images in healthy volunteers, consisting of cold and warm data sets for each individual, were considered satisfactory ($n = 5$) to excellent ($n = 3$). Of the two volunteers who reported a history of cold sensitivity, one had a history of fingertip cyanosis generalized to all digits on cold exposure. In this subject, four segments were visualized when subjected to cold challenge; this increased to 14 segments after warming. In the second subject, who gave a history of left thumb cold sensitivity manifesting as blanching and nail bed cyanosis, 14 segments were visualized when cold, increasing to 17 with warming. Beading of the princeps pollicis artery was also apparent in this subject and persisted after warming (Fig 5).

In the patient group, image quality was considered satisfactory (with warming) and excellent (with cooling) in one patient and poor in the other two patients. Fewer segments were visualized overall. The first patient, who had a history of right index finger amputation for ischemic gangrene and chronic right middle fingertip ulceration, had nine arterial segments visualized with cooling; eight segments were visualized after warming (Fig 6). Of the patients with poor image quality, the first was in atrial fibrillation at imaging; seven segments were visualized, increasing to eight segments with warming. The superficial and deep palmar arches and the princeps pollicis artery were well seen, with poor conspicuity of the visualized common and proper digital arteries. Motion artifact limited the interpretation of images of both palmar and digital segments. The last patient had frequent ventricular ectopic beats, reported discomfort with lateral decubitus positioning, and had evidence of bulk motion on images. However, the deep arch and princeps pollicis artery were visualized at both cool and warm imaging, without alteration in the number of visualized segments or their caliber.

Discussion

Contrast-enhanced MR angiography of the hands is widely acknowledged as chal-

lenging owing to the competing demands of high spatial resolution and short arteriovenous transit time, which constrains the overall acquisition time (20). Venous contamination in particular has been problematic, with use of centric reordering timed to optimal arterial opacification (21), timed arterial compression (5), and subsystolic cuff compression advocated as means of minimizing venous overlay. Although not ideal, contrast-enhanced MR angiography has been preferred to traditional unenhanced techniques and to phase-contrast and time-of-flight MR angiography, which suffer from long acquisition times for comparable spatial reso-

lution. Relatively slow flow and in-plane saturation offer challenges for time-of-flight imaging, and appropriate velocity encoding selection is a concern for phase-contrast MR angiography (1).

In our early experience, VFA MR angiography offers the opportunity for unenhanced pure arterial imaging. Because it is a subtraction technique, background signal is suppressed. It is relatively rapid, with submillimeter in-plane resolution imaging achievable in approximately 3 minutes. It is well tolerated, particularly when subjects are imaged in the lateral decubitus position, and allows for repeated studies if there is motion artifact or if temperature challenge is desirable. Decreased radiofrequency deposition with the VFA approach permits efficient imaging at 3.0 T. The high signal-to-noise ratio available with 3.0-T imaging can be directly translated into improved spatial resolution,

Figure 2

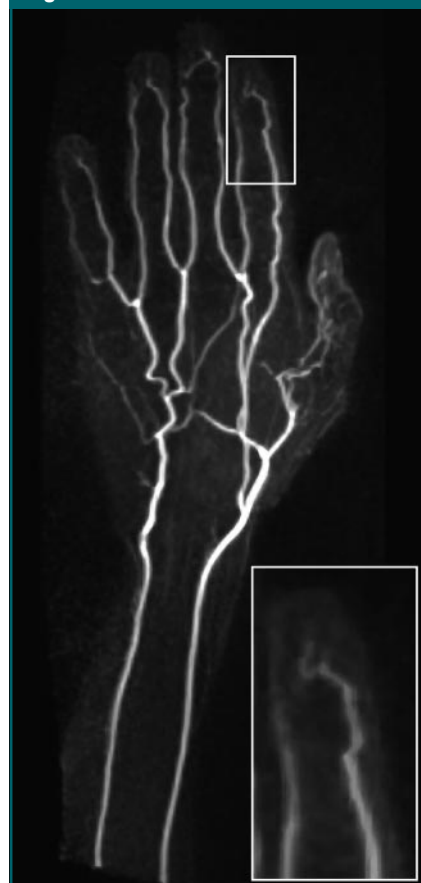


Figure 2: Coronal subtraction MIP VFA MR angiogram (repetition time, two R-R intervals; echo time, 10 msec; variable flip angle) of left hand of 45-year-old man (healthy volunteer) clearly depicts the hand arteries, including the terminal nutrient arteries. The inset is a magnified image of the distal left index finger and nutrient vessels.

Figure 3

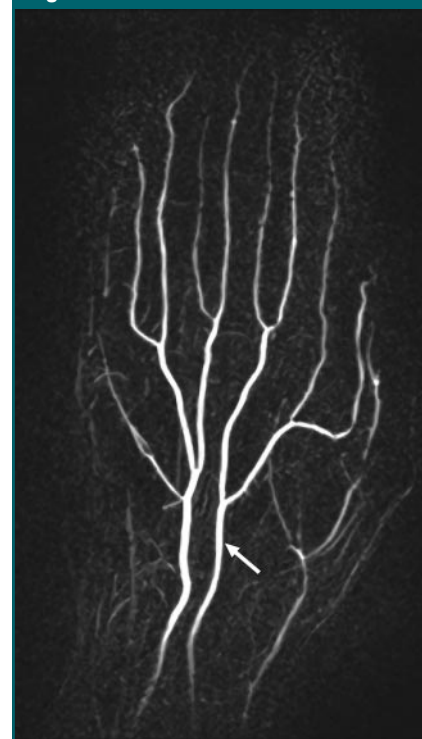


Figure 3: Coronal subtraction MIP VFA MR angiogram (repetition time, two R-R intervals; echo time, 10 msec; variable flip angle) of left hand of 38-year-old woman (healthy volunteer). Variant arterial anatomy, with a persistent median artery (arrow), is depicted.

with high conspicuity of the proper digital arteries in our series and visualization of the terminal nutrient arteries in three subjects.

Application of partial Fourier or parallel imaging techniques in the phase-encoding direction enables shorter echo train lengths and readout duration, mini-

mizing vessel blur and maintaining clear demarcation between systolic and diastolic acquisitions. A segmented acquisition was used to further minimize readout

Figure 4

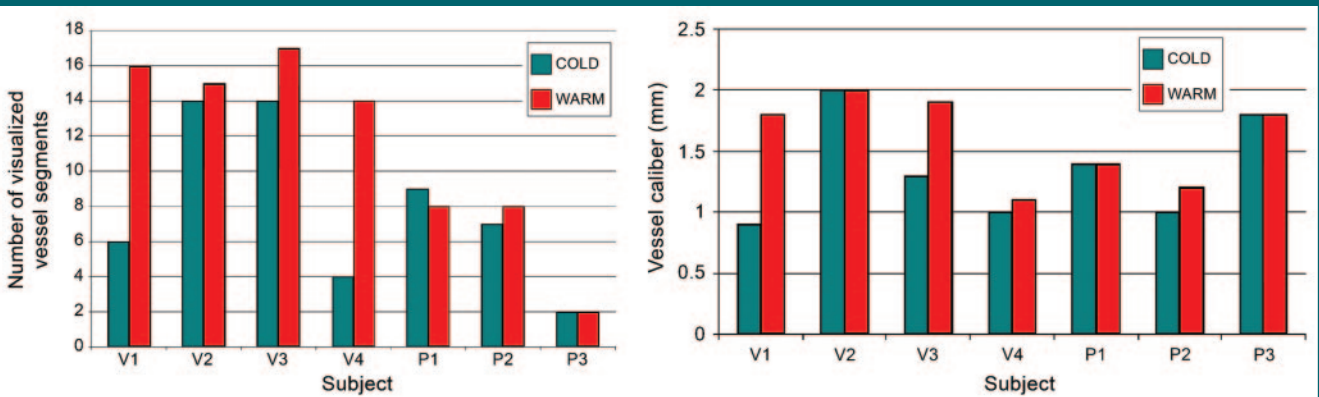


Figure 4: Results of provocative temperature challenge in seven subjects. **(a)** Graph shows number of visualized vessel segments per hand in volunteers (*V*) and patients (*P*). Note the increase in the number of visualized segments on warming observed in healthy volunteers, compared with a minimal change in the patient subgroup. **(b)** Graph shows caliber of a representative vessel in the hand of each subject. The terminal radial artery was measured for patient 3 (*P3*), and the superficial arch was measured in all other subjects, at identical positions on cold and warm images. An increase in vessel caliber was observed in three volunteers (*V*) and one patient (*P*).

Figure 5

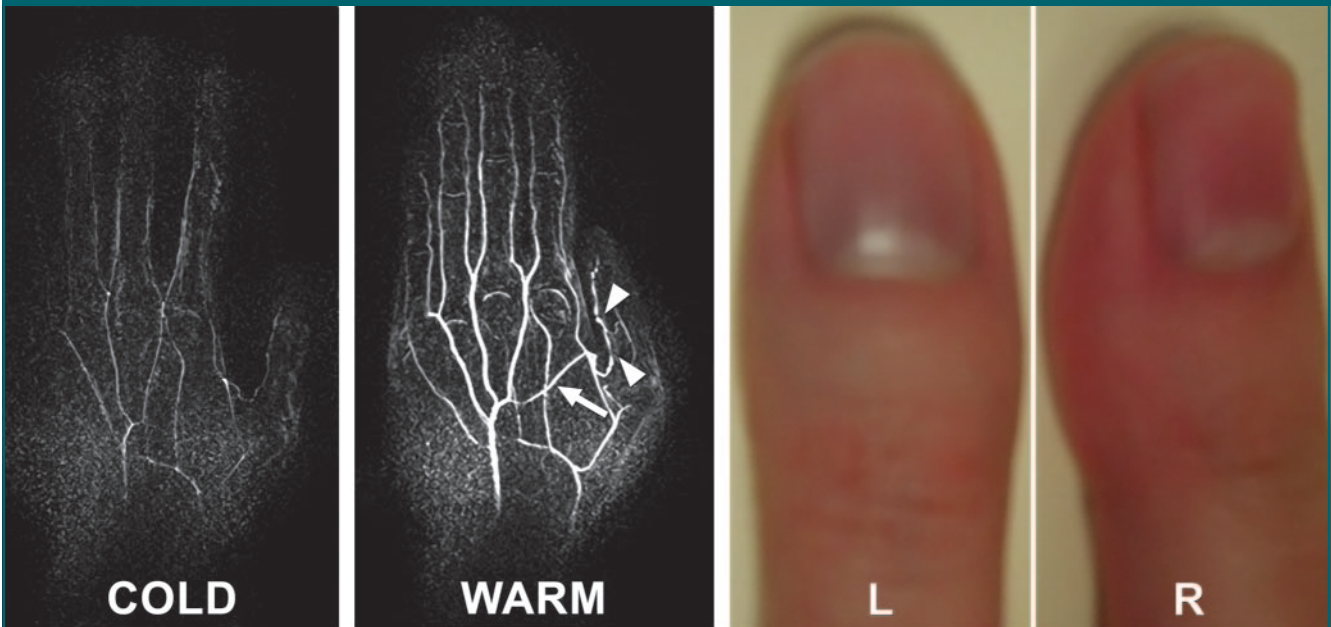


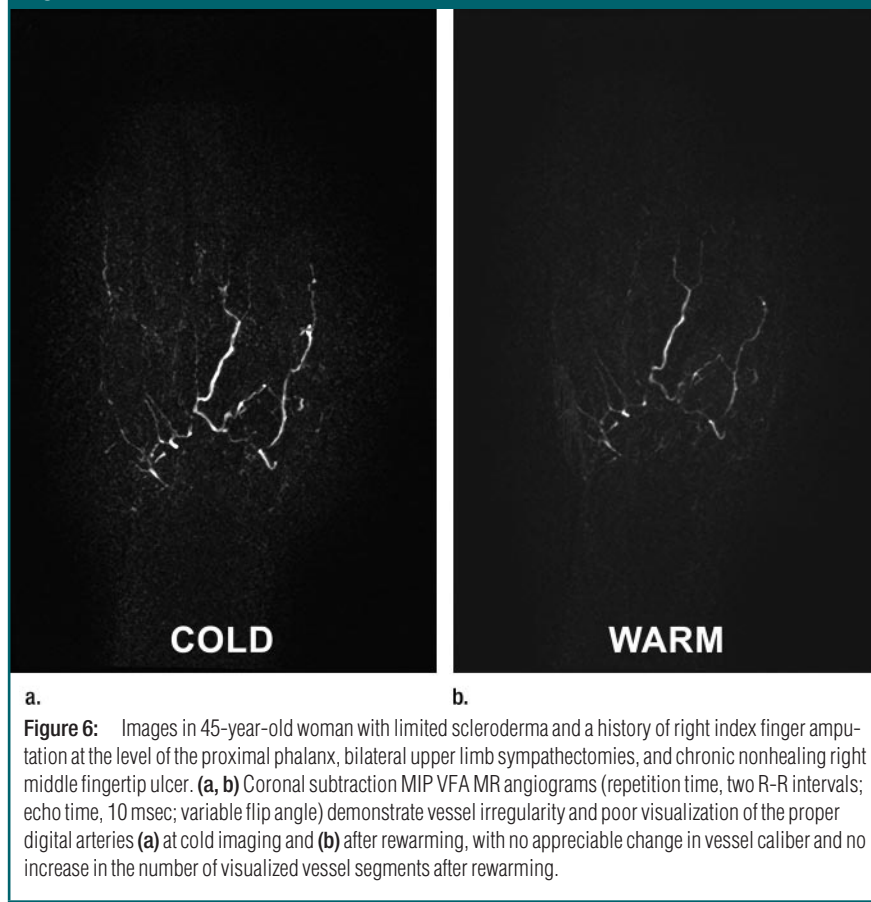
Figure 5: Images in 34-year-old female volunteer with a history of cold sensitivity localized to the left thumb (blanching and cyanosis). **(a, b)** Coronal subtraction MIP VFA MR angiograms (repetition time, two R-R intervals; echo time, 10 msec; variable flip angle) obtained after **(a)** cooling and **(b)** rewarming. Cold challenge resulted in small vessel caliber and poor visualization of the proper digital arteries. Increased vessel diameter and completion of the superficial arch (arrow) are noted on warming. Note the presence of princeps pollicis beading with focal stenoses (arrowheads). **(c)** Photographs obtained after the cold challenge show the subject's pale blue left (*L*) thumb nailbed and normal right (*R*) thumb for comparison.

duration in our series because the differentiation of systolic and diastolic flow is particularly important in the hand, where peak systolic velocities are as low as 23 cm/sec \pm 12 for healthy subjects (22) and may potentially be even lower when vasculopathy is present.

We also noted marked changes in vessel segment visualization and conspicuity after cold challenge and warming in healthy subjects, including the two “healthy” volunteers with clinical symptoms and examination findings of fingertip blanching and cyanosis at cold exposure. Conversely, little change in vessel visualization was observed in a small population of patients with scleroderma. Cold stress testing and rewarming have previously been used to evaluate patients with primary and secondary Raynaud phenomenon with a variety of techniques, including Doppler ultrasonography (US) (23,24), where decreases in digital and palmar arch velocity, with increases in resistive and pulsatility indexes, were demonstrated in patients with Raynaud phenomenon compared with healthy control subjects. However, Doppler US is operator dependent and subject to acoustic window limitations. Contrast-enhanced MR angiography can provide a high-spatial-resolution, reliable anatomic assessment, as has been shown without provocative testing in scleroderma (25,26).

Unenhanced MR angiography offers the added advantage of consistently pure arterial phase imaging, allowing provocative testing within a single visit. In systemic scleroderma, where secondary Raynaud phenomenon is the presenting feature in more than 90% of patients (27), endothelial dysfunction leads to structural changes in the vessel wall that are not seen in patients with primary Raynaud phenomenon (27). Fixed versus reversible vascular abnormalities can be potentially visualized, enabling simultaneous anatomic and functional evaluation. Reliable evaluation of the presence and degree of reversibility could provide a biomarker for differentiating primary from secondary Raynaud phenomenon. With the development of medical therapies targeting the endothelium, including endothelin receptor antagonists and α 2c-

Figure 6



a. **b.**
Figure 6: Images in 45-year-old woman with limited scleroderma and a history of right index finger amputation at the level of the proximal phalanx, bilateral upper limb sympathectomies, and chronic nonhealing right middle fingertip ulcer. **(a, b)** Coronal subtraction MIP VFA MR angiograms (repetition time, two R-R intervals; echo time, 10 msec; variable flip angle) demonstrate vessel irregularity and poor visualization of the proper digital arteries **(a)** at cold imaging and **(b)** after rewarming, with no appreciable change in vessel caliber and no increase in the number of visualized vessel segments after rewarming.

adrenoceptor antagonists (27,28), there is exciting potential to evaluate the efficacy of therapeutic regimens in the population of patients with scleroderma.

Our results are preliminary and illustrate the promising nature of this unenhanced MR angiography method for imaging hand vessels. The main limitation of our work was the lack of an imaging standard for comparison. Because vasculopathy may decrease differences between systolic and diastolic velocities, this could adversely affect vessel visualization with a flow-dependent technique such as ours, leading to disease overestimation—especially in the patient group. In addition, a standardized cooling technique was not employed, and this could partially account for some of the observed differences between volunteers and patients subjected to temperature provocation. Further evaluation of the technique in a larger clinical population and with digital

subtraction angiography validation is required.

Exploring the effect of cardiac arrhythmias on image quality is also warranted. Inaccurate triggering could cause inappropriate fast flow dephasing in some k-space partitions of the “diastolic” acquisition. Similarly, it could cause bright signal from slow flow in some k-space partitions of the “systolic” acquisition. Such inconsistencies in k-space will corrupt the reconstruction of the arteries on both image sets, causing signal loss and incoherent artifacts on the subtracted images. Inaccurate triggering could also cause variations in the degree of T1 relaxation between consecutive readout periods, which may contribute to incomplete background suppression. Additional future work includes development of a custom-designed hand coil by using elements of appropriate size and with optimized sensitivity profiles, engendering further

gains in spatial resolution and imaging speed. More aggressive k-space under-sampling techniques, particularly parallel imaging, could be explored, enabling a single-shot acquisition with a minimized acquisition window. This could potentially also increase the robustness of the sequence for arrhythmias.

Three-dimensional electrocardiographically gated unenhanced VFA MR angiography of the hands enables clear separation of veins from arteries, with high in-plane resolution and excellent small vessel conspicuity. The technique can be repeated multiple times in a single session without the use of intravenous contrast material, with potential clinical application in the assessment of vascular reactivity with warming and cooling, such as with the Raynaud phenomenon in a population of patients with connective tissue disease.

Acknowledgment: The authors thank Martha Helmers, BS, for her expert assistance with preparation of the figures.

References

- Rofsky NM. MR angiography of the hand and wrist. *Magn Reson Imaging Clin N Am* 1995; 3:345–359.
- Loring LA, Hallisey MJ. Arteriography and interventional therapy for diseases of the hand. *RadioGraphics* 1995;15:1299–1310.
- Connell DA, Koulouris G, Thorn DA, Potter HG. Contrast-enhanced MR angiography of the hand. *RadioGraphics* 2002;22:583–599.
- Lee VS, Lee HM, Rofsky NM. Magnetic resonance angiography of the hand: a review. *Invest Radiol* 1998;33:687–698.
- Wentz KU, Frohlich JM, von Weymarn C, Patak MA, Jenelten R, Zollkofer CL. High-resolution magnetic resonance angiography of hands with timed arterial compression (tac-MRA). *Lancet* 2003;361:49–50.
- Brauck K, Maderwald S, Vogt FM, Zenge M, Barkhausen J, Herborn CU. Time-resolved contrast-enhanced magnetic resonance angiography of the hand with parallel imaging and view sharing: initial experience. *Eur Radiol* 2007;17:183–192.
- Grobner T. Gadolinium: a specific trigger for the development of nephrogenic fibrosing dermopathy and nephrogenic systemic fibrosis? *Nephrol Dial Transplant* 2006;21:1104–1108.
- Krause U, Pabst T, Kenn W, Wittenberg G, Hahn D. MR angiography of the hand arteries. *Angiology* 2001;52:763–772.
- Wedeen VJ, Meuli RA, Edelman RR, et al. Projective imaging of pulsatile flow with magnetic resonance. *Science* 1985;230:946–948.
- Miyazaki M, Sugiura S, Tateishi F, Wada H, Kassai Y, Abe H. Non-contrast-enhanced MR angiography using 3D ECG-synchronized half-Fourier fast spin echo. *J Magn Reson Imaging* 2000;12:776–783.
- Lim RP, Hecht EM, Xu J, et al. 3D nongadolinium-enhanced ECG-gated MRA of the distal lower extremities: preliminary clinical experience. *J Magn Reson Imaging* 2008;28:181–189.
- Mugler JPI, Meyer H, Kiefer B. Practical implementation of optimized tissue-specific prescribed signal evolutions for improved turbo-spin-echo imaging [abstr]. In: Proceedings of the Eleventh Meeting of the International Society for Magnetic Resonance in Medicine. Berkeley, Calif: International Society for Magnetic Resonance in Medicine, 2003; 203.
- Xu J, Weale P, Laub G, et al. A novel non-contrast MR angiography technique using triggered non-selective refocused SPACE for improved spatial resolution and speed [abstr]. In: Proceedings of the Sixteenth Meeting of the International Society for Magnetic Resonance in Medicine. Berkeley, Calif: International Society for Magnetic Resonance in Medicine, 2008; 730.
- Miyazaki M, Lee VS. Nonenhanced MR angiography. *Radiology* 2008;248:20–43.
- Griswold MA, Jakob PM, Heidemann RM, et al. Generalized autocalibrating partially parallel acquisitions (GRAPPA). *Magn Reson Med* 2002;47:1202–1210.
- Miyazaki M, Takai H, Sugiura S, Wada H, Kuwahara R, Urata J. Peripheral MR angiography: separation of arteries from veins with flow-spoiled gradient pulses in electrocardiography-triggered three-dimensional half-Fourier fast spin-echo imaging. *Radiology* 2003;227:890–896.
- Atanasova IP, Storey P, Lim RP, et al. Effect of flip angle evolution on flow sensitivities in ECG-gated fast spin echo MRA methods at 3T [abstr]. In: Proceedings of the Seventeenth Meeting of the International Society for Magnetic Resonance in Medicine. Berkeley, Calif: International Society for Magnetic Resonance in Medicine, 2009; 422.
- Busse RF. Flow sensitivity of CPMG sequences with variable flip refocusing and implications for CSF signal uniformity in 3D-FSE imaging [abstr]. In: Proceedings of the Fourteenth Meeting of the International Society for Magnetic Resonance in Medicine. Berkeley, Calif: International Society for Magnetic Resonance in Medicine, 2006; 2430.
- Gluecker TM, Bongartz G, Ledermann HP, Bilecen D. MR angiography of the hand with subsystolic cuff-compression optimization of injection parameters. *AJR Am J Roentgenol* 2006;187:905–910.
- Goldfarb JW, Hochman MG, Kim DS, Edelman RR. Contrast-enhanced MR angiography and perfusion imaging of the hand. *AJR Am J Roentgenol* 2001;177:1177–1182.
- Winterer JT, Scheffler K, Paul G, et al. Optimization of contrast-enhanced MR angiography of the hands with a timing bolus and elliptically reordered 3D pulse sequence. *J Comput Assist Tomogr* 2000;24:903–908.
- Trager S, Pignataro M, Anderson J, Kleinert JM. Color flow Doppler: imaging the upper extremity. *J Hand Surg [Am]* 1993;18:621–625.
- Chikui T, Izumi M, Eguchi K, Kawabe Y, Nakamura T. Doppler spectral waveform analysis of arteries of the hand in patients with Raynaud's phenomenon as compared with healthy subjects. *AJR Am J Roentgenol* 1999;172:1605–1609.
- Naidu S, Baskerville PA, Goss DE, Roberts VC. Raynaud's phenomenon and cold stress testing: a new approach. *Eur J Vasc Surg* 1994;8:567–573.
- Allanore Y, Seror R, Chevrot A, Kahan A, Drape JL. Hand vascular involvement assessed by magnetic resonance angiography in systemic sclerosis. *Arthritis Rheum* 2007; 56:2747–2754.
- Wang J, Yarnykh VL, Molitor JA, et al. Micro magnetic resonance angiography of the finger in systemic sclerosis. *Rheumatology (Oxford)* 2008;47:1239–1243.
- Sunderkotter C, Riemekasten G. Pathophysiology and clinical consequences of Raynaud's phenomenon related to systemic sclerosis. *Rheumatology (Oxford)* 2006;45(suppl 3): iii33–iii35.
- Hennes S, Wigley FM. Current drug therapy for scleroderma and secondary Raynaud's phenomenon: evidence-based review. *Curr Opin Rheumatol* 2007;19:611–618.

Radiology 2009

This is your reprint order form or pro forma invoice

(Please keep a copy of this document for your records.)

Reprint order forms and purchase orders or prepayments must be received 72 hours after receipt of form either by mail or by fax at 410-820-9765. It is the policy of Cadmus Reprints to issue one invoice per order.

Please print clearly.

Author Name _____
Title of Article _____
Issue of Journal _____ Reprint # _____ Publication Date _____
Number of Pages _____ KB# _____ Symbol Radiology
Color in Article? Yes / No (Please Circle)

Please include the journal name and reprint number or manuscript number on your purchase order or other correspondence.

Order and Shipping Information

Reprint Costs (Please see page 2 of 2 for reprint costs/fees.)

_____ Number of reprints ordered \$ _____
_____ Number of color reprints ordered \$ _____
_____ Number of covers ordered \$ _____
Subtotal \$ _____
Taxes \$ _____

(Add appropriate sales tax for Virginia, Maryland, Pennsylvania, and the District of Columbia or Canadian GST to the reprints if your order is to be shipped to these locations.)

First address included, add \$32 for
each additional shipping address \$ _____

TOTAL \$ _____

Shipping Address (cannot ship to a P.O. Box) Please Print Clearly

Name _____
Institution _____
Street _____
City _____ State _____ Zip _____
Country _____
Quantity _____ Fax _____
Phone: Day _____ Evening _____
E-mail Address _____

Additional Shipping Address* (cannot ship to a P.O. Box)

Name _____
Institution _____
Street _____
City _____ State _____ Zip _____
Country _____
Quantity _____ Fax _____
Phone: Day _____ Evening _____
E-mail Address _____

* Add \$32 for each additional shipping address

Payment and Credit Card Details

Enclosed: Personal Check _____
Credit Card Payment Details _____
Checks must be paid in U.S. dollars and drawn on a U.S. Bank.
Credit Card: VISA Am. Exp. MasterCard
Card Number _____
Expiration Date _____
Signature: _____

Please send your order form and prepayment made payable to:

Cadmus Reprints

P.O. Box 751903

Charlotte, NC 28275-1903

Note: Do not send express packages to this location, PO Box.

FEIN #: 541274108

Signature _____ Date _____

Signature is required. By signing this form, the author agrees to accept the responsibility for the payment of reprints and/or all charges described in this document.

Invoice or Credit Card Information

Invoice Address Please Print Clearly

Please complete Invoice address as it appears on credit card statement

Name _____
Institution _____
Department _____
Street _____
City _____ State _____ Zip _____
Country _____
Phone _____ Fax _____
E-mail Address _____

Cadmus will process credit cards and Cadmus Journal Services will appear on the credit card statement.

If you don't mail your order form, you may fax it to 410-820-9765 with your credit card information.

Radiology 2009

Black and White Reprint Prices

Domestic (USA only)						
# of Pages	50	100	200	300	400	500
1-4	\$239	\$260	\$285	\$303	\$323	\$340
5-8	\$379	\$420	\$455	\$491	\$534	\$572
9-12	\$507	\$560	\$651	\$684	\$748	\$814
13-16	\$627	\$698	\$784	\$868	\$954	\$1,038
17-20	\$755	\$845	\$947	\$1,064	\$1,166	\$1,272
21-24	\$878	\$985	\$1,115	\$1,250	\$1,377	\$1,518
25-28	\$1,003	\$1,136	\$1,294	\$1,446	\$1,607	\$1,757
29-32	\$1,128	\$1,281	\$1,459	\$1,632	\$1,819	\$2,002
Covers	\$149	\$164	\$219	\$275	\$335	\$393

Color Reprint Prices

Domestic (USA only)						
# of Pages	50	100	200	300	400	500
1-4	\$247	\$267	\$385	\$515	\$650	\$780
5-8	\$297	\$435	\$655	\$923	\$1194	\$1467
9-12	\$445	\$563	\$926	\$1,339	\$1,748	\$2,162
13-16	\$587	\$710	\$1,201	\$1,748	\$2,297	\$2,843
17-20	\$738	\$858	\$1,474	\$2,167	\$2,846	\$3,532
21-24	\$888	\$1,005	\$1,750	\$2,575	\$3,400	\$4,230
25-28	\$1,035	\$1,164	\$2,034	\$2,986	\$3,957	\$4,912
29-32	\$1,186	\$1,311	\$2,302	\$3,402	\$4,509	\$5,612
Covers	\$149	\$164	\$219	\$275	\$335	\$393

International (includes Canada and Mexico)						
# of Pages	50	100	200	300	400	500
1-4	\$299	\$314	\$367	\$429	\$484	\$546
5-8	\$470	\$502	\$616	\$722	\$838	\$949
9-12	\$637	\$687	\$852	\$1,031	\$1,190	\$1,369
13-16	\$794	\$861	\$1,088	\$1,313	\$1,540	\$1,765
17-20	\$963	\$1,051	\$1,324	\$1,619	\$1,892	\$2,168
21-24	\$1,114	\$1,222	\$1,560	\$1,906	\$2,244	\$2,588
25-28	\$1,287	\$1,412	\$1,801	\$2,198	\$2,607	\$2,998
29-32	\$1,441	\$1,586	\$2,045	\$2,499	\$2,959	\$3,418
Covers	\$211	\$224	\$324	\$444	\$558	\$672

International (includes Canada and Mexico)						
# of Pages	50	100	200	300	400	500
1-4	\$306	\$321	\$467	\$642	\$811	\$986
5-8	\$387	\$517	\$816	\$1,154	\$1,498	\$1,844
9-12	\$574	\$689	\$1,157	\$1,686	\$2,190	\$2,717
13-16	\$754	\$874	\$1,506	\$2,193	\$2,883	\$3,570
17-20	\$710	\$1,063	\$1,852	\$2,722	\$3,572	\$4,428
21-24	\$1,124	\$1,242	\$2,195	\$3,231	\$4,267	\$5,300
25-28	\$1,320	\$1,440	\$2,541	\$3,738	\$4,957	\$6,153
29-32	\$1,498	\$1,616	\$2,888	\$4,269	\$5,649	\$7,028
Covers	\$211	\$224	\$324	\$444	\$558	\$672

Minimum order is 50 copies. For orders larger than 500 copies, please consult Cadmus Reprints at 800-407-9190.

Reprint Cover

Cover prices are listed above. The cover will include the publication title, article title, and author name in black.

Shipping

Shipping costs are included in the reprint prices. Domestic orders are shipped via FedEx Ground service. Foreign orders are shipped via a proof of delivery air service.

Multiple Shipments

Orders can be shipped to more than one location. Please be aware that it will cost \$32 for each additional location.

Delivery

Your order will be shipped within 2 weeks of the journal print date. Allow extra time for delivery.

Tax Due

Residents of Virginia, Maryland, Pennsylvania, and the District of Columbia are required to add the appropriate sales tax to each reprint order. For orders shipped to Canada, please add 7% Canadian GST unless exemption is claimed.

Ordering

Reprint order forms and purchase order or prepayment is required to process your order. Please reference journal name and reprint number or manuscript number on any correspondence. You may use the reverse side of this form as a proforma invoice. Please return your order form and prepayment to:

Cadmus Reprints
P.O. Box 751903
Charlotte, NC 28275-1903

Note: Do not send express packages to this location, PO Box. FEIN #: 541274108

Please direct all inquiries to:

Rose A. Baynard
800-407-9190 (toll free number)
410-819-3966 (direct number)
410-820-9765 (FAX number)
baynardr@cadmus.com (e-mail)

Reprint Order Forms and purchase order or prepayments must be received 72 hours after receipt of form.